

Robust Visual Object Tracking with Natural Language Region Proposal Network

Qi Feng¹, Vitaly Ablavsky¹, Qinxun Bai², and Stan Sclaroff¹

¹Department of Computer Science, Boston University

²Horizon Robotics

¹{fung,ablavsky,sclaroff}@bu.edu

²qinxun.bai@gmail.com

Abstract

Tracking with natural-language (NL) specification is a powerful new paradigm to yield trackers that initialize without a manually-specified bounding box, stay on target in spite of occlusions, and auto-recover when diverged. These advantages stem in part from visual appearance and NL having distinct and complementary invariance properties. However, realizing these advantages is technically challenging: the two modalities have incompatible representations. In this paper, we present the first practical and competitive solution to the challenge of tracking with NL specification. Our first novelty is an NL region proposal network (NL-RPN) that transforms an NL description into a convolutional kernel and shares the search branch with siamese trackers; the combined network can be trained end-to-end. Secondly, we propose a novel formulation to represent the history of past visual exemplars and use those exemplars to automatically reset the tracker together with our NL-RPN. Empirical results over tracking benchmarks with NL annotations demonstrate the effectiveness of our approach.

1 Introduction

“A picture is worth a thousand words” goes an old adage. Thus, a typical approach to tracking requires a “picture” called an *exemplar* to initialize tracking [7, 12, 26]. Even tracking methods that self-initialize via a proposal mechanism, be it motion-detection or a class-specific detector, use the proposal to obtain a “picture” of the object to be tracked.

As new applications of computer-vision gain prominence, the validity of that old adage becomes less obvious. Broadly, these new applications are unified by an idea of “AI you can talk to.” In this paper, we develop a new formulation, in effect betting that “a few words are worth a thousand pixels.” We opt for a natural-language (NL) description of the target.

However, conditioning a tracker on NL description is not straightforward. First, since tracking implies temporal coherence, applying an algorithm for matching text to image regions [37, 40] for each video frame independently would not yield competitive results in challenging scenarios. Second, it is not obvious how to derive a formulation to combine the strengths of appearance-based

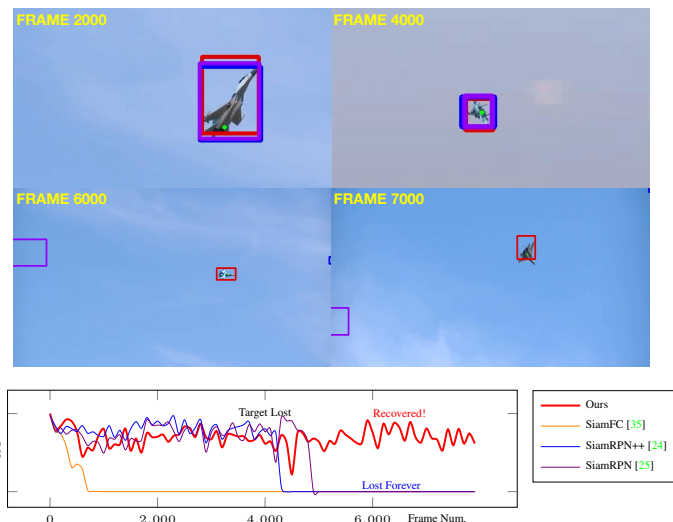


Figure 1: With the proposed Natural Language Region Proposal Network (NL-RPN) and Memory Management Mechanism (MMM), presented in Fig. 2 and Alg. 2, our siamese based tracker recovers from target loss and model drift better than competing siamese trackers. In this example we show the Intersection over Union (IoU) between the ground truth and each trackers’ predictions as plotted against frame numbers. Siamese trackers are not capturing temporal variation of the target, which causes target to be lost. With the help of the proposed NL-RPN and MMM, our tracker is better at automatically recover from losses of target and occlusions, as shown in Tbl. 2.

tracking with the language modality. Indeed, the best published attempts [13, 26] did not fare well compared to the state-of-the-art in visual tracking benchmarks. In this paper, we propose a natural language region proposal network (NL-RPN) to perform tracking by NL description.

In contrast with prior NL-tracking work, we exploit a siamese tracking by detection architecture. However, past siamese trackers [24, 25, 35] have modeled little or no temporal variations of targets [15]. Therefore, we propose a memory management mechanism (MMM) algorithm, which is implemented as a state machine [39] to update the visual *exemplar* of the target and thereby enable siamese trackers to capture the temporal variations of the

target.

As a result of the proposed NL-RPN and MMM algorithm, we build a tracker that is able to recover from model drift by automatically resetting itself using the NL description of the target. An example of such a recovery is shown in Fig. 1.

Contributions of this paper include the following:

- A novel natural language region proposal network (NL-RPN) that performs tracking by consuming video sequence and a natural-language description of the target to be tracked. Specifically, this is the first siamese correlation filter based tracker that consumes NL instead of region templates.
- We propose a Memory Management Mechanism (MMM) for tracking, which not only handles the visual exemplar updates used in the proposed tracker, but also makes online decisions about tracking state transitions as well. The MMM makes it possible to restore the proposed tracker based on its own history of decisions. Compared to past siamese trackers, our tracker is more robust in recovering from occlusions and target losses.
- The proposed NL-RPN is end-to-end trained offline with large scale training set of image sentence pairs. Experiments on visual object tracking benchmarks that are annotated with NL shows that our tracker is more robust in terms of recovering from occlusions and target losses.

2 Related Works

2.1 Tracking

In the past two decades, tracking by detection models [3, 20] and Bayesian filtering based algorithms [4, 21] have been thoroughly studied in the field of visual object tracking. Some deep learning based models [2, 7, 30, 34] have been introduced in recent years, and are argued to perform better when handling occlusion and appearance change. ECO [7] applies convolutional filters on convolution feature maps to obtain satisfactory performance on multiple tracking datasets. ECO still suffers from efficiency issues [17], though its efficiency is improved from the original convolution filter based tracker, C-COT [8]. These trackers maintain appearance and motion models explicitly by maintaining the visual features over time. SiamFC [2] conducts a local search for regions with a similar regional visual features obtained by a CNN in every frame. SiamRPN [25] and SiamRPN++ [24] performs tracking as one shot detection using the siamese network as a region proposal network. However, these siamese trackers do not model the temporal appearance variations of the target and have model drift problems.

2.2 Language Understanding in Vision Tasks

In the last decade, researchers start to look into exploiting natural language understanding in vision tasks. These models usually consist of two components: a language model and an appearance model to learn a new feature space that is shared between both NL

and appearance [19, 36]. Li *et al.* define two tracking by natural language specification problems [26]. Feng *et al.* formalize the tracking by natural language in a tracking by detection framework with Bayesian detection formulation [13]. However, in their work, an assumption that appearances and the natural language description be conditional independent given the bounding boxes is made. By directly measuring this joint conditional probability, we derive a fully convolutional neural network (CNN) that performs tracking by natural language description. Similar to that of Li *et al.*'s work [25], we formulate the tracking with natural language description problem as one-shot detection.

3 Natural Language Region Proposal Network (NL-RPN)

Following [13] and [35], let I_t denote the frame from a sequence at time step t , and let Q be the NL description of the target. Variables and functions used in deriving the proposed tracker are summarized in Table 1. Rather than assume conditional independence between target appearance and Q given the ground truth bounding box [13], we propose a Natural Language Region Proposal Network (NL-RPN), which estimates the conditional probability $\Pr[\mathbb{A}_t|X_t, Q]$, where \mathbb{A}_t is a set of anchor boxes and X_t represents the search patch at time step t .

The overall architecture of our model is presented in Fig. 2. The NL-RPN takes NL description of the target and performs detection on the search patch, while the Siamese Region Proposal Network (SiamRPN) [25] takes a visual exemplar and performs detection on the same search patch. Both RPNs share the same backbone CNN, which makes the proposed model fully convolutional and therefore compatible with past siamese trackers, in particular, our model can be combined with SiamRPN and trained jointly end-to-end.

In this section, we describe our proposed one-shot detection model using NL description of the target. We present our tracker using this one-shot detection model later in Sec. 4.

3.1 Architecture of NL-RPN

The architecture of the NL-RPN is shown in the top half of Fig. 2. We designed the NL-RPN to be fully convolutional and compatible with siamese trackers.

As is common practice, the NL description Q is transformed into an embedding using a sentence embedding model [1, 5, 31] pretrained on a text corpus. Our novelty is the follow-on transformation from this sentence embedding into an *NL kernel* denoted by Z_Q followed by 1×1 convolution layers, denoted as ϕ_{cls} and ϕ_{reg} . These convolutional layers, ϕ_{cls} and ϕ_{reg} , turn Z_Q into a tensor compatible with X_t for the depth-wise cross correlation layer to estimate the target score and regression for all anchor boxes:

$$\begin{aligned} \mathbb{A}_t^{Z_Q, \text{cls}} &= v_{\text{cls}}(\psi(X_t)) \star \phi_{\text{cls}}(Z_Q); \\ \mathbb{A}_t^{Z_Q, \text{reg}} &= v_{\text{reg}}(\psi(X_t)) \star \phi_{\text{reg}}(Z_Q), \end{aligned} \quad (1)$$

Variable	Definition
t, t_i, t_j	Time indices.
I_t	Frame at time step t .
X_t	The search patch at time step t .
Q	The NL description of target.
Z_Q	NL kernel learned from embedding of Q .
Z_{t_i}	The visual exemplar at time t_i .
\mathbb{Z}	The memory, $\{Z_{t_1}, \dots, Z_{t_M}\}$.
\mathbb{A}_t	A set of anchor boxes.
\mathbb{B}_t	Bounding boxes regressed from \mathbb{A}_t .
\mathbb{S}_t	Corresponding positive scores for \mathbb{A}_t .
$\hat{\mathbb{B}}_t$	Predicted bounding box at time t .
$\hat{\mathbb{S}}_t$	The positive score of $\hat{\mathbb{B}}_t$.
ψ	Siamese convolutional neural networks.
φ, v, ϕ	1x1 convolutional layers.
\star	Depth-wise cross correlation layers.
χ	Discrete tracking state.

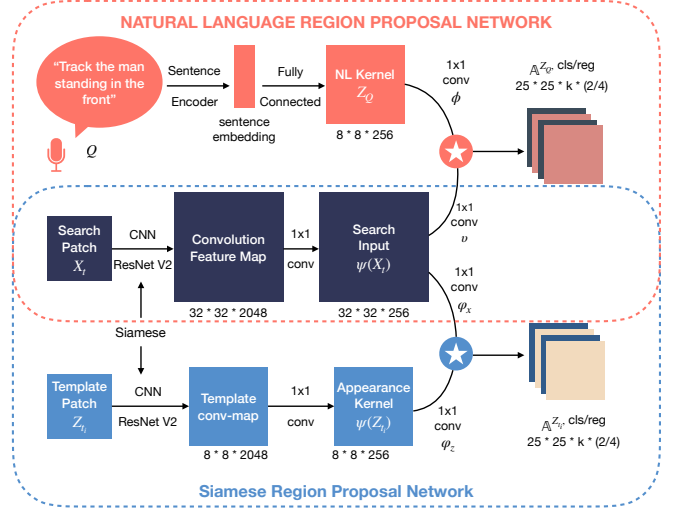


Table 1: Notations of variables and neural networks used in deriving the proposed NL-RPN and tracker.

where v_{cls} and v_{reg} are multiple 1×1 convolution layers with batch normalization on the convolutional feature map of X_t . The tensor $\mathbb{A}_t^{Z_Q, \text{cls}}$ have a shape of $w \times h \times 2k$ and $\mathbb{A}_t^{Z_Q, \text{reg}}$ have a shape of $w \times h \times 4k$, where w, h are width and height of the convolution feature map and k is the number of anchors. We consider Eq. 1 as an estimation of probabilities for anchor boxes: $\Pr[\mathbb{A}_t|X_t, Q]$.

Furthermore, if visual exemplars are available for our proposed tracker, a SiamRPN [24] based detector, shown in the bottom half of Fig. 2, is utilized to further assist the NL-RPN. Let $\mathbb{Z} = \{Z_{t_1}, \dots, Z_{t_M}\}$ be a set of visual exemplars of the target at earlier time steps seen by the tracker, *i.e.*, $t_1, \dots, t_M < t$. The siamese CNN ψ is used to extract appearance features from these visual exemplars. Additional convolutional layers together with batch normalization, φ_{cls} and φ_{reg} are finally used to estimate the joint probability $\Pr[\mathbb{A}_t|X_t, Z_{t_i}]$ for each visual exemplar $Z_{t_i} \in \mathbb{Z}$:

$$\begin{aligned} \mathbb{A}_t^{Z_{t_i}, \text{cls}} &= \varphi_{\text{cls}, x}(\psi(X_t)) \star \varphi_{\text{cls}, z}(\psi(Z_{t_i})); \\ \mathbb{A}_t^{Z_{t_i}, \text{reg}} &= \varphi_{\text{reg}, x}(\psi(X_t)) \star \varphi_{\text{reg}, z}(\psi(Z_{t_i})). \end{aligned} \quad (2)$$

We describe how to use both the NL-RPN and the SiamRPN with \mathbb{Z} to perform tracking in Sec. 4.

3.2 Loss Functions and Training

As the proposed NL-RPN is fully convolutional and shares the same backbone with the SiamRPN, the NL-RPN can be trained either jointly with the SiamRPN or it can be trained after the SiamRPN is trained, both in an end-to-end fashion. To construct training instances that resemble the test-time distribution, we randomly choose two frames at different time steps, I_{t_i} and I_{t_j} , together with the corresponding ground truth bounding boxes $B_{t_i}^*$ and $B_{t_j}^*$. We crop and resize Z_{t_i} (on I_{t_i}) for the visual exemplar,

Figure 2: The proposed model - the NL-RPN is shown in the magenta box and the SiamRPN is shown in the blue box. The NL-RPN takes NL description of the target and performs a detection based on the search patch, while SiamRPN exploits visual cues from visual exemplars. Additionally, the NL-RPN and the SiamRPN shares the same network for the search patch, which makes the proposed model fully convolutional and fully compatible with a wide range of siamese trackers. Finally, the NL-RPN is trained end-to-end together with SiamRPN with triplets of visual exemplar, NL description and search patch as described in Sec. 3.2.

and X_{t_j} (on I_{t_j}) for the search patch. Thus, a triplet (Z_{t_i}, X_{t_j}, Q) , is constructed as the input for training our proposed tracker.

Similar to the training process of the RPN in Faster RCNN [14], we sample 16 anchors that have an intersection over union (IoU) with $B_{t_j}^*$ greater than 0.7 as positive anchors and another 48 anchors that have an IoU less than 0.3 as negative anchors. We use a softmax cross entropy loss for training *classification* branches and a smoothed $L1$ -loss, for training *regression* branches in both the NL-RPN and the SiamRPN.

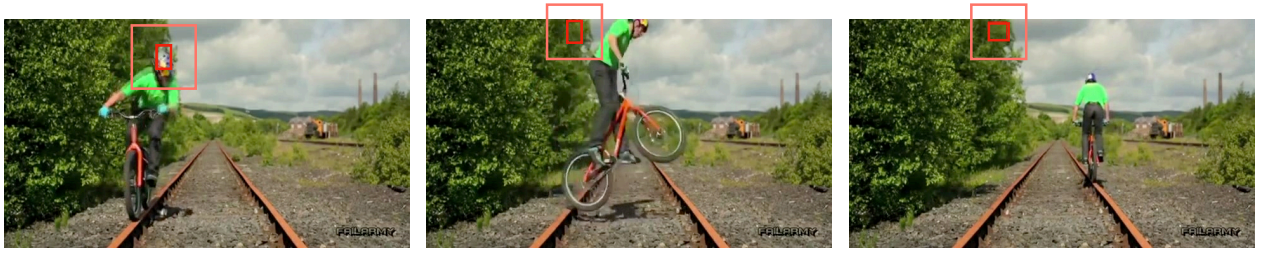
4 Tracking with NL-RPN

In this section, we will discuss how to use a trained NL-RPN to perform tracking with NL description. Alg. 1 shows the proposed tracking algorithm.

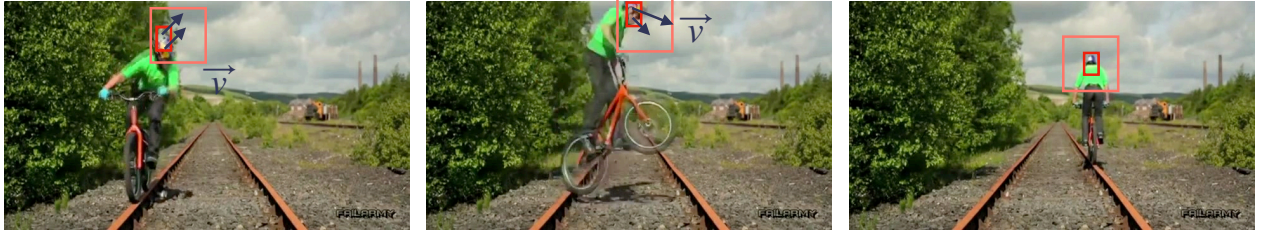
4.1 Initialization

While initializing \mathbb{Z} in our tracker with a ground truth bounding box B_1^* is straightforward, initializing it with Q when B_1^* is not available is non-trivial.

The scale of the target, *i.e.*, the relative size of the target with respect to the frame, is essential for the proposed tracker to work, as NL-RPN and SiamRPN are trained with anchors of fixed scales. When initializing with NL only, we adopt sliding windows search



Without Optical Flow Guidance, targets that are moving rapidly will move outside of the search patch X_t .



Using the average optical flow \vec{v} within \hat{B}_{t-1} , the target is more likely to be covered by the search patch X_t .

Figure 3: With the help with optical flow for motion guidance, a better sampling strategy for X_t gives NL-RPN and Siamese RPN a higher chance of making the correct prediction.

for an initial bounding box \hat{B}_1 with highest prediction confidence from NL-RPN given the scale of the target.

the NL-RPN denoted as $\mathbb{S}_t^Z, \mathbb{B}_t^Z$ and $\mathbb{S}_t^{Z_Q}, \mathbb{B}_t^{Z_Q}$ respectively:

$$\begin{aligned} \mathbb{S}_t^Z &\doteq \sigma \left(\mathbb{A}_t^{Z, \text{cls}} \right), \mathbb{S}_t^{Z_Q} \doteq \sigma \left(\mathbb{A}_t^{Z_Q, \text{cls}} \right); \\ \mathbb{B}_t^Z &\doteq \text{BOX REGRESSION} \left(\mathbb{A}_t^{Z, \text{reg}} \right); \\ \mathbb{B}_t^{Z_Q} &\doteq \text{BOX REGRESSION} \left(\mathbb{A}_t^{Z_Q, \text{reg}} \right). \end{aligned} \quad (4)$$

4.2 Sampling X_t with Optical Flow Guidance

It has become standard practice to adopt a *constant position* motion model and to search for the target in a new frame I_t in a region centered at the previous predicted location \hat{B}_{t-1} . However, such search strategy is sub-optimal as it ignores both the target’s motion and the global scene motion. As is shown in Fig. 3, this sampling strategy would end up with target loss and would make neither the NL-RPN nor the SiamRPN able to make correct detection.

Therefore, we use the average optical flow within \hat{B}_{t-1} predicted by FlowNet 2 [18] as guidance for cropping X_t from I_t . Following the guidance of the motion, X_t is cropped on the center of \hat{B}_{t-1} adding the average optical flow \vec{v} .

A sub-window attention function, g , with a 2D-Gaussian function centered at X_t is used to boost scores of anchors near the center of X_t and reduce scores of anchors distant from the center of X_t . Therefore, for both SiamRPN and NL-RPN, we choose the bounding box with the highest score:

$$\begin{aligned} \hat{S}_t^Z &\doteq \left(\mathbb{S}_t^Z \right)_m; & \hat{S}_t^{Z_Q} &\doteq \left(\mathbb{S}_t^{Z_Q} \right)_n; \\ \hat{B}_t^Z &\doteq \left(\mathbb{B}_t^Z \right)_m; & \hat{B}_t^{Z_Q} &\doteq \left(\mathbb{B}_t^{Z_Q} \right)_n, \end{aligned} \quad (5)$$

$$m = \arg \max_{S_m \in \mathbb{S}_t^Z} g(S_m), \quad n = \arg \max_{S_n \in \mathbb{S}_t^{Z_Q}} g(S_n). \quad (6)$$

4.3 Detection with NL-RPN and SiamRPN

After obtaining the search patch X_t , we run an inference pass of the proposed model to obtain $\mathbb{A}_t^{Z, \text{cls}}, \mathbb{A}_t^{Z, \text{reg}}, \mathbb{A}_t^{Z_Q, \text{cls}}$, and $\mathbb{A}_t^{Z_Q, \text{reg}}$. In practice, when tracking with multiple visual exemplars, our tracker choose the visual exemplar with the highest positive score for any anchor for making inference:

$$\mathbb{A}_t^{Z, \text{cls}} \doteq \mathbb{A}_t^{\hat{Z}_t, \text{cls}}, \quad \mathbb{A}_t^{Z, \text{reg}} \doteq \mathbb{A}_t^{\hat{Z}_t, \text{reg}}, \quad (3)$$

where $\hat{Z}_t = \arg \max_{Z \in \mathbb{Z}} \left(\max_{w, h, k} \sigma \left(\mathbb{A}_t^{Z, \text{cls}} \right)_{w, h, k} \right)$, σ is the function that applies the softmax activation and extracts the value for the foreground class.

By resizing $\mathbb{A}_t^{Z, \text{cls}}, \mathbb{A}_t^{Z_Q, \text{cls}}$ and applying the regression, we get a set of bounding boxes and scores proposed by the SiamRPN and

4.4 Memory Management Mechanism (MMM)

The proposed Memory Management Mechanism (MMM) is designed for extra robustness of the proposed tracker. There are two major functionalities of the MMM: 1). Capture the temporal appearance variation of the target in Memory \mathbb{Z} ; 2). Determine the state of tracking, denoted as χ . MMM is presented in Alg. 2, and the transition of tracking state χ is shown in Fig. 4.

Initialize \mathbb{Z} : We first initialize \mathbb{Z} from either a ground truth bounding box B_1^* or an estimation \hat{B}_1 from Q as described in Sec. 4.1. Afterwards, at time step t , when an inference is made, either from the NL-RPN or the SiamRPN, the predicted bounding box \hat{B}_t is

Algorithm 1: The proposed tracker.

Input : I_1, \dots, I_T, Z_Q , and optionally B_1^* .

if B_1^* is given **then**
 | $\hat{B}_1 = B_1^*$
else
 | $\hat{B}_1 =$ Multi-scale sliding window search from NL-RPN
 | with Z_Q and I_1
end

Initialize $\mathbb{Z} = \{Z_1\}$
State $\chi = STABLE$

for $t = 2$ **to** T **do**
 | Sample X_t with Optical Flow Guidance
 | // Make Prediction Following Eq. 5.
 | **if** $\chi \neq CONTINUED\ LOST$ **then**
 | | $\hat{S}_t, \hat{B}_t =$ SIAMRPN(X_t, \mathbb{Z})
 | **else**
 | | $\hat{S}_t, \hat{B}_t =$ NL-RPN(X_t, Z_Q)
 | **end**
 | // Run MMM algorithm as in Alg. 2.
 | $\chi, \mathbb{Z} =$ MMM($\{\hat{S}_1, \dots, \hat{S}_t\}, \hat{B}_t$)
end

Output: $\hat{B}_1, \dots, \hat{B}_T$.

used to sample a new visual exemplar Z_t and add it to the memory of the tracker \mathbb{Z} if certain criteria are met.

Updating \mathbb{Z} by Reverse Nearest Neighbor: Intuitively, we wish to only add confident predictions into the memory. However, having redundant visual exemplars not only slows down the tracker, but also makes the tracker become biased and eventually drift away from the target. Therefore, we adopt the reverse nearest neighbor algorithm [22, 32] and add Z_t to \mathbb{Z} if the reverse nearest neighbor set of Z_t with \mathbb{Z} is an empty set. The rationale is that we add Z_t to \mathbb{Z} only if the new exemplar “looks” different to its past, and therefore the memory captures the temporal appearance variations of the target.

Each exemplar Z_t is given an initial weight as $Z_t^w = 1.0$, when added to \mathbb{Z} . Z_t^w will decrease if it does not achieve the highest score in Eq. 3 for every time step and will increase otherwise. Similar to the halving algorithm [28], if the weight become less than 0, the corresponding Z_{t_i} will be removed from \mathbb{Z} .

In practice, in order to make the memory efficient, the proposed tracker only runs reverse nearest neighbor every $\Delta T = 50$ frames and only if the score \hat{S}_t is higher than a threshold of $\tau_1 = 0.99$.

Tracking State χ : With the history of decisions $\hat{S}_1, \dots, \hat{S}_{t-1}$ made during inference, the proposed tracker makes a decision on which of the following four state it would be in: 1. *Stable* 2. *Lost* 3. *Continued Lost* 4. *Restore* The transition criteria of these four states are presented in Fig. 4. The tracking state transition is implemented as a rule based state machine, similar to that of Xiang *et al.*’s work [39].

Stable means that our tracker is confident about its decisions.

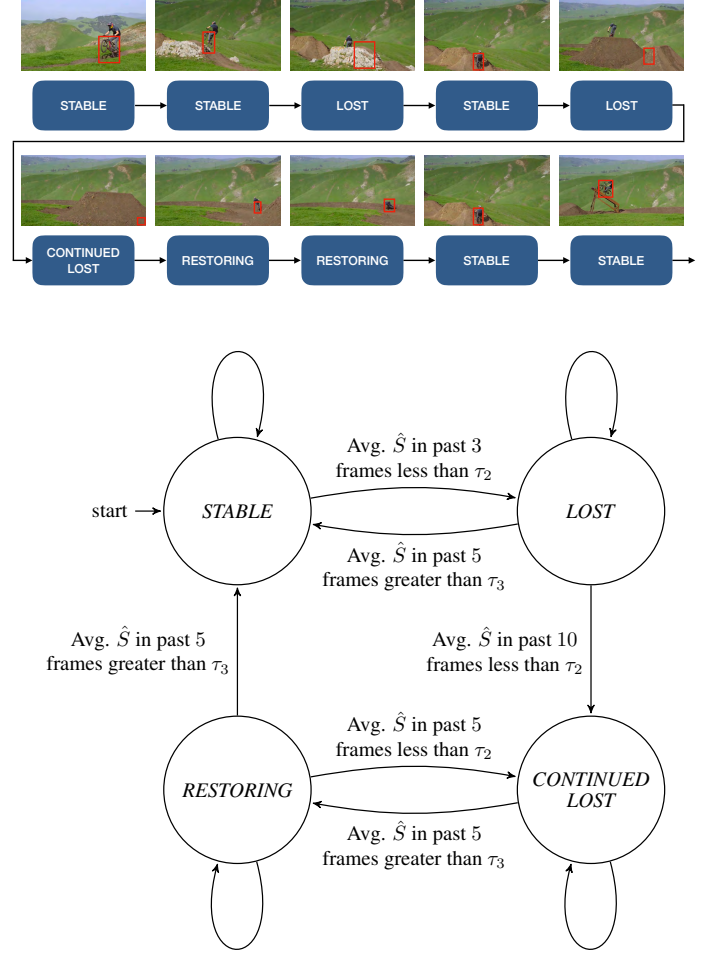


Figure 4: Transition of tracking states used in the proposed Memory Management Mechanism with an example on *bicycle-18* video from LaSOT [11] dataset.

Lost means that our tracker is not confident about its recent decisions, *i.e.*, scores from immediate past $\hat{S}_t, \hat{S}_{t-1}, \hat{S}_{t-2}$ are lower than a threshold of τ_2 and the target might have lost the search region X_t . Although this might be due to an appearance change or partial occlusion of the target, our tracker will rely on the NL-RPN for making decisions and the sub-window attention function g is no longer used during inference.

However, if the model transits into the *Continued Lost* state, it means that the tracker has been suffering from a long-term lost of the target, *i.e.*, scores in a longer immediate past is lower than the threshold τ_2 . In this case, we restore the tracker to a historical state in the memory to handle scale changes of the target. Additionally, in order to handle appearance changes or occlusion for an extended period of time, we utilize the proposed NL-RPN to automatically “reset” the tracker, which will be discussed in details in Sec. 4.5. After the model is restored from *Continued Lost* state, it enters a state called *Restore*. If the proposed tracker is stable for a period of time, it will eventually get back to the *Stable* state. On the other hand, if the model starts to make low confident predictions in a

Algorithm 2: Memory Management Mechanism (MMM).

Input : $\chi, Z_t, \mathbb{Z}, \{\hat{S}_1, \dots, \hat{S}_t\}, \tau_1, \tau_2, \tau_3$.
Update χ as in Fig. 4 with $\{\hat{S}_1, \dots, \hat{S}_t\}, \tau_2, \tau_3$
for Z_i **in** \mathbb{Z} **do**
 Find \hat{Z}_t according to Eq. 3.
 if $Z_i = \hat{Z}_t$ **then**
 $Z_i^w = Z_i^w - 0.2$
 else
 $Z_i^w = Z_i^w + 1$
 end
end
if $t \equiv 0 \pmod{25}$ **and** $\chi = STABLE$ **then**
 if $\frac{1}{\Delta T} \sum_{i=t-\Delta T-1}^t \hat{S}_i > \tau_1$ **then**
 Add Z_t to \mathbb{Z} using Reverse Nearest Neighbor Algorithm
 end
 for Z_i **in** \mathbb{Z} **do**
 if $Z_i^w < 0$ **then**
 $\mathbb{Z} = \mathbb{Z} \setminus \{Z_i\}$
 end
 end
end
Output: updated χ and \mathbb{Z} .

Restore state, it will switch back to the *Continued Lost* State.

4.5 NL-RPN and SiamRPN Aggregation

The proposed NL-RPN is used to “reset” the tracker when the MMM determines that the model is in the *Lost* or *Continued Lost* state.

A naive approach to aggregate NL-RPN with SiamRPN would be a weighted sum following a similar mechanism from SiamRPN++ [24]. However, this is not well motivated, as the two modalities of visual appearance and natural language generate different kernels for the depth-wise cross correlation operation; indeed this approach does not fare well on our datasets.

Therefore, as discussed earlier, our proposed NL-RPN is used for only making decisions when our tracker enters the *Lost* or *Continued Lost* state. Our tracker performs an automatic reset by the NL-RPN with Q and X_t sampled on I_t with multiple scales (sizes) and locations based on visual exemplars \mathbb{Z} .

5 Experiments

In this section, we first describe the datasets used in our experiments and show the effectiveness of our proposed NL-RPN and MMM by conducting a comprehensive set of ablation studies. Then, we compare our tracker with other state-of-the-art visual object trackers and past NL trackers.

5.1 Datasets

5.1.1 Training Datasets

Our backbone ResNet [16] model is pretrained on ImageNet [9]. We use all images and phrases from VisualGenome [23], frames from MSCOCO [27] and YouTube-BoundingBox [33], together with images and phrases from training splits of LaSOT and lang-OTB-99 [26] for training the SiamRPN backbone and NL-RPN. We choose to follow [24] to choose the size of 127×127 pixels for Z_{t_i} and the size of 255×255 pixels for X_{t_j} during training.

5.1.2 Evaluation Datasets

With the tracking by NL setup, we are aware of two publicly available tracking benchmarks that are **annotated with NL** for targets. In Li *et al.*’s early work on NL tracking [26], they annotated OTB-100 [38] with NL and end up with a Lingual OTB99 dataset. In a more recent work [11], LaSOT, a large single object tracking benchmark dataset annotated with NL for targets, is introduced with 70 different categories of objects and 20 sequences for each category, totaling at 1,400 sequences. We choose to follow the protocol 2 from the original publication, which is to evaluate our tracking by One Pass Evaluation (OPE) on the testing split of the dataset.

5.2 Implementation Details

5.2.1 Training Initialization

We initialize the stride-reduced ResNet [24] with pretrained weights on ImageNet [9] and randomly initialize layers in the SiamRPN following the original work [25]. Layers other than the sentence encoder in the proposed NL-RPN are initialized randomly to construct the NL kernel described in Sec. 3.1. The sentence encoder is implemented via a universal sentence encoder [6].

5.2.2 Learning Rates and Convergence

We train our proposed NL-RPN together with SiamRPN using a TensorFlow 2.0 implementation on 4 Nvidia Titan V GPUs with Adagrad [10] optimizer and an initial learning rate at 0.001. We decay the learning rate after 5 epochs to 0.0005 and continued training for another 5 epochs. Batch size is set to 16 per GPU for a total of 64 triplets of Z_{t_i} , X_{t_j} , and Q per batch. Gradients are averaged over each batch, while the gradients for NL-RPN are omitted if Q is not present. The proposed model takes about 2 days to converge using the loss described in Sec. 3.2.

5.3 Comparisons with Siamese Baseline

In this section, we conduct comprehensive experiments and ablation study comparing the performance of three variants of our proposed tracker with the strong baseline of SiamRPN++ [24] tracker.

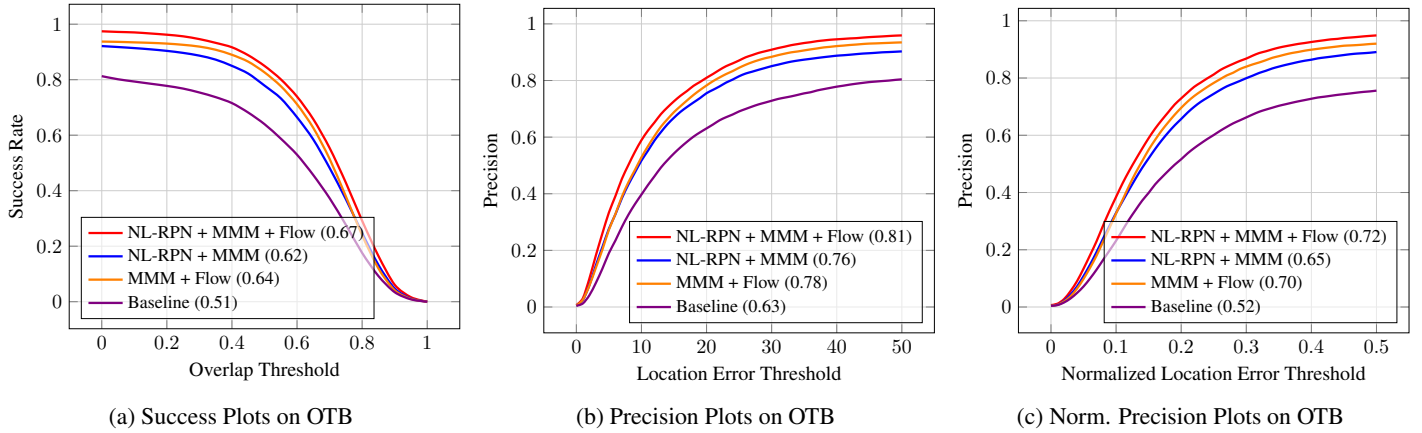


Figure 5: Ablation studies on the OTB-99-language dataset using the OPE protocol. The Baseline is our re-implementation of SiamRPN++ [24]. NL-RPN+MMM+Flow is the full-fledged version of our tracker. NL-RPN+MMM and MMM+Flow are two simplified variants of our tracker, with the optical flow-guided sampling (Flow) component and the NL-RPN component removed respectively.

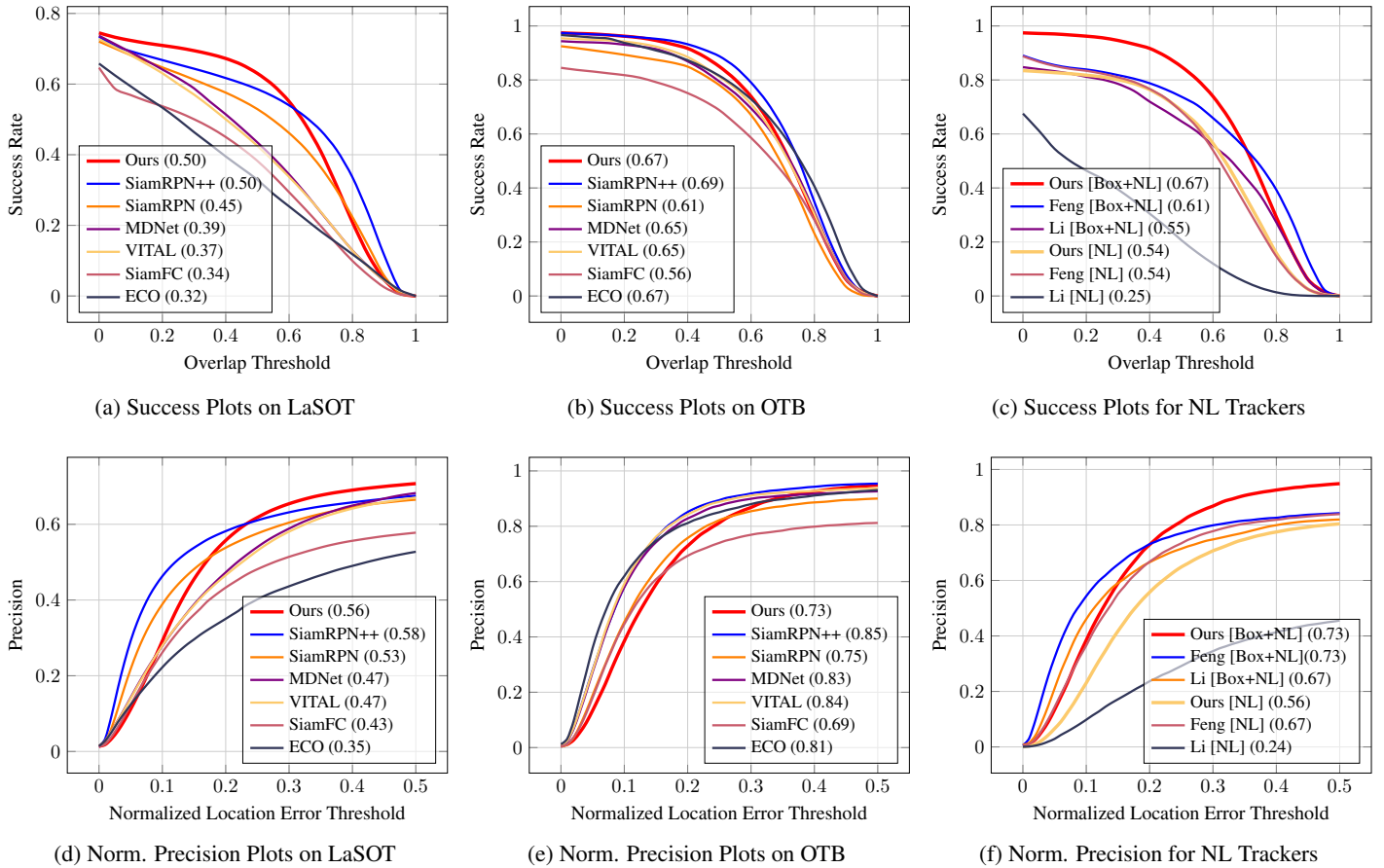


Figure 6: Comparison of our approach against state-of-the-art traditional trackers and NL trackers: AUC of success rate at different intersection over union thresholds and AUC of mean average precision at different location error thresholds on testing videos in LaSOT and OTB-99-lang.

Tracker	[1]↑	[2]↓	[3]↓
Ours	0.149	371.56	60.05
SiamRPN++ [24]	0.134	467.92	110.95
SiamRPN [25]	0.127	413.52	109.50
MDNet [29]	0.148	394.00	86.06
VITAL [34]	0.143	437.58	85.05
SiamFC [35]	0.077	618.91	151.90
ECO [7]	0.123	464.39	107.78

[1] Avg. IoU in 100 consecutive frames after occlusions;

[2] Avg. num. of frames until recover (IoU > 0) after occlusions;

[3] Avg. num. of frames until recover (IoU > 0) after lost of targets (IoU = 0).

↑: Higher the better; ↓: Lower the better.

Table 2: With the proposed NL-RPN and MMM, our tracker is able to recover from occlusions and target loss faster than other trackers on LaSOT [11].

OPE results on the OTB-99-language dataset are shown in Fig. 5.¹ The proposed new mechanisms, NL-RPN and MMM, effectively boost the tracking performance of the Siamese baseline by a large margin, and the adoption of optical flow-guided sampling strategy lead to further performance boost.

5.4 Comparisons with Other Trackers

We also compare our proposed model with the following state-of-the-art trackers: SiamRPN++ [24], SiamRPN [25], MDNet [29], VITAL [34], SiamFC [2], ECO [7], Li [26], and Feng [13]. For the fairness of comparison, we use their released codes, model weights, and hyper-parameters in all experiments.

In Fig. 6, we plot the success rate at different IoU thresholds and the precision at different location error thresholds on both LaSOT [11] and OTB-99-lang [26]. We also report the area under curve (AUC) for each plotted curve. In Fig. 6c and Fig. 6f, we follow Li *et al.* [26] to conduct experiments on OTB-lang-99 under two different setups for tracking with NL, *i.e.*, tracking with NL only and initialization with both the bounding box and the NL description of the target. Overall, our tracker is competitive with state-of-the-art trackers and NL trackers.

Moreover, to validate the ability of our proposed tracker in recovering from occlusions and loss of target during tracking, we compute the following statistics from the OPE (starting from the first frame) on LaSOT: 1) Average IoU with ground truth bounding box on 100 consecutive frames after each full occlusion; 2) Average number of frames until a tracker is able to reacquire the target with an IoU greater than 0 after each full occlusion; and 3) Average number of frames until a tracker is able to reacquire the target with an IoU greater than 0 after each target loss (no intersection between prediction and ground truth). The results are summarized in Table 2. Our tracker is able to recover from occlusions and target

¹We re-implement the SiamRPN++ and train it from scratch. While we were not able to reproduce the performance of the released model (after hyper-parameter tuning), we use the same set of hyper-parameters for all variants of our tracker and thus enables a fair comparison between the baseline and our methods.

losses faster than all competing trackers, which demonstrates the effectiveness and strength of the proposed NL-RPN and MMM.

6 Conclusion

We present a novel NL-RPN which performs tracking by consuming video sequence and an NL description of the target. Together with the proposed MMM for tracking, our tracker enjoys better robustness than other visual object trackers. Experiments on challenging datasets demonstrate that our tracker is better at handling occlusions and recovering from lost of targets than other state-of-the-art trackers and prior attempts on NL tracking.

References

- [1] Yoshua Bengio, Réjean Ducharme, Pascal Vincent, and Christian Jauvin. A neural probabilistic language model. *Journal of Machine Learning Research*, 3(Feb):1137–1155, 2003. 2
- [2] Luca Bertinetto, Jack Valmadre, João F Henriques, Andrea Vedaldi, and Philip HS Torr. Fully-convolutional siamese networks for object tracking. *arXiv preprint arXiv:1606.09549*, 2016. 2, 8
- [3] Samuel S Blackman. Multiple hypothesis tracking for multiple target tracking. *IEEE Aerospace and Electronic Systems Magazine*, 19(1):5–18, 2004. 2
- [4] Eli Brookner. g–h and g–h–k filters. *Tracking and Kalman Filtering Made Easy*, pages 3–63. 2
- [5] Andrea Burns, Reuben Tan, Kate Saenko, Stan Sclaroff, and Bryan A Plummer. Language features matter: Effective language representations for vision-language tasks. In *Proceedings of the IEEE International Conference on Computer Vision*, pages 7474–7483, 2019. 2
- [6] Daniel Cer, Yinfei Yang, Sheng-yi Kong, Nan Hua, Nicole Limtiaco, Rhomni St John, Noah Constant, Mario Guajardo-Cespedes, Steve Yuan, Chris Tar, et al. Universal sentence encoder. *arXiv preprint arXiv:1803.11175*, 2018. 6
- [7] Martin Danelljan, Goutam Bhat, Fahad Shahbaz Khan, and Michael Felsberg. Eco: Efficient convolution operators for tracking. In *Proceedings of the IEEE Conference on Computer Vision and Pattern Recognition*, pages 6638–6646, 2017. 1, 2, 8
- [8] Martin Danelljan, Andreas Robinson, Fahad Shahbaz Khan, and Michael Felsberg. Beyond correlation filters: Learning continuous convolution operators for visual tracking. In *European Conference on Computer Vision*, pages 472–488. Springer, 2016. 2
- [9] Jia Deng, Wei Dong, Richard Socher, Li-Jia Li, Kai Li, and Li Fei-Fei. Imagenet: A large-scale hierarchical image database. In *2009 IEEE Conference on Computer Vision and Pattern Recognition*, pages 248–255. Ieee, 2009. 6
- [10] John Duchi, Elad Hazan, and Yoram Singer. Adaptive subgradient methods for online learning and stochastic optimization. *Journal of Machine Learning Research*, 12(Jul):2121–2159, 2011. 6
- [11] Heng Fan, Liting Lin, Fan Yang, Peng Chu, Ge Deng, Sijia Yu, Hexin Bai, Yong Xu, Chunyuan Liao, and Haibin Ling. Lasot: A high-quality benchmark for large-scale single object tracking. In *Proceedings of the IEEE Conference on Computer Vision and Pattern Recognition*, pages 5374–5383, 2019. 5, 6, 8

- [12] Christoph Feichtenhofer, Axel Pinz, and Andrew Zisserman. Detect to track and track to detect. In *Proceedings of the IEEE International Conference on Computer Vision*, pages 3038–3046, 2017. 1
- [13] Qi Feng, Vitaly Ablavsky, Qinxun Bai, Guorong Li, and Stan Sclaroff. Tell me what to track. *arXiv preprint arXiv:1907.11751*, 2019. 1, 2, 8
- [14] Ross Girshick. Fast r-cnn. In *Proceedings of the IEEE International Conference on Computer Vision*, pages 1440–1448, 2015. 3
- [15] Qing Guo, Wei Feng, Ce Zhou, Rui Huang, Liang Wan, and Song Wang. Learning dynamic siamese network for visual object tracking. In *Proceedings of the IEEE International Conference on Computer Vision*, pages 1763–1771, 2017. 1
- [16] Kaiming He, Xiangyu Zhang, Shaoqing Ren, and Jian Sun. Identity mappings in deep residual networks. In *European Conference on Computer Vision*, pages 630–645. Springer, 2016. 6
- [17] Chen Huang, Simon Lucey, and Deva Ramanan. Learning policies for adaptive tracking with deep feature cascades. In *Proceedings of the IEEE International Conference on Computer Vision*, pages 105–114, 2017. 2
- [18] Eddy Ilg, Nikolaus Mayer, Tonmoy Saikia, Margret Keuper, Alexey Dosovitskiy, and Thomas Brox. FlowNet 2.0: Evolution of optical flow estimation with deep networks. In *Proceedings of the IEEE Conference on Computer Vision and Pattern Recognition*, pages 2462–2470, 2017. 4
- [19] Justin Johnson, Andrej Karpathy, and Li Fei-Fei. Denscap: Fully convolutional localization networks for dense captioning. In *Proceedings of the IEEE Conference on Computer Vision and Pattern Recognition*, pages 4565–4574, 2016. 2
- [20] Zdenek Kalal, Krystian Mikolajczyk, and Jiri Matas. Tracking-learning-detection. *IEEE Transactions on Pattern Analysis and Machine Intelligence*, 34(7):1409–1422, 2012. 2
- [21] Rudolph Emil Kalman et al. A new approach to linear filtering and prediction problems. *Journal of Basic Engineering*, 82(1):35–45, 1960. 2
- [22] Flip Korn, S. Muthukrishnan, and S. Muthukrishnan. Influence sets based on reverse nearest neighbor queries. In *Proceedings of the 2000 ACM SIGMOD International Conference on Management of Data*, SIGMOD '00, pages 201–212, New York, NY, USA, 2000. ACM. 5
- [23] Ranjay Krishna, Yuke Zhu, Oliver Groth, Justin Johnson, Kenji Hata, Joshua Kravitz, Stephanie Chen, Yannis Kalantidis, Li-Jia Li, David A Shamma, et al. Visual genome: Connecting language and vision using crowdsourced dense image annotations. *International Journal of Computer Vision*, 123(1):32–73, 2017. 6
- [24] Bo Li, Wei Wu, Qiang Wang, Fangyi Zhang, Junliang Xing, and Junjie Yan. Siamrpn++: Evolution of siamese visual tracking with very deep networks. In *Proceedings of the IEEE Conference on Computer Vision and Pattern Recognition*, pages 4282–4291, 2019. 1, 2, 3, 6, 7, 8
- [25] Bo Li, Junjie Yan, Wei Wu, Zheng Zhu, and Xiaolin Hu. High performance visual tracking with siamese region proposal network. In *Proceedings of the IEEE Conference on Computer Vision and Pattern Recognition*, pages 8971–8980, 2018. 1, 2, 6, 8
- [26] Zhenyang Li, Ran Tao, Efstratios Gavves, Cees GM Snoek, and Arnold WM Smeulders. Tracking by natural language specification. In *Proceedings of the IEEE Conference on Computer Vision and Pattern Recognition*, pages 6495–6503, 2017. 1, 2, 6, 8
- [27] Tsung-Yi Lin, Michael Maire, Serge Belongie, James Hays, Pietro Perona, Deva Ramanan, Piotr Dollár, and C Lawrence Zitnick. Microsoft coco: Common objects in context. In *European Conference on Computer Vision*, pages 740–755. Springer, 2014. 6
- [28] Nick Littlestone. Learning quickly when irrelevant attributes abound: A new linear-threshold algorithm. *Machine learning*, 2(4):285–318, 1988. 5
- [29] Hyeonseob Nam and Bohyung Han. Learning multi-domain convolutional neural networks for visual tracking. In *Proceedings of the IEEE Conference on Computer Vision and Pattern Recognition*, pages 4293–4302, 2016. 8
- [30] Guanghan Ning, Zhi Zhang, Chen Huang, Xiaobo Ren, Haohong Wang, Canhui Cai, and Zhihai He. Spatially supervised recurrent convolutional neural networks for visual object tracking. In *2017 IEEE International Symposium on Circuits and Systems (ISCAS)*, pages 1–4. IEEE, 2017. 2
- [31] Jeffrey Pennington, Richard Socher, and Christopher Manning. Glove: Global vectors for word representation. In *Proceedings of the 2014 Conference on Empirical Methods in Natural Language Processing (EMNLP)*, pages 1532–1543, 2014. 2
- [32] Federico Pernici, Federico Bartoli, Matteo Bruni, and Alberto Del Bimbo. Memory based online learning of deep representations from video streams. In *Proceedings of the IEEE Conference on Computer Vision and Pattern Recognition*, pages 2324–2334, 2018. 5
- [33] Esteban Real, Jonathon Shlens, Stefano Mazzocchi, Xin Pan, and Vincent Vanhoucke. Youtube-boundingboxes: A large high-precision human-annotated data set for object detection in video. In *Proceedings of the IEEE Conference on Computer Vision and Pattern Recognition*, pages 5296–5305, 2017. 6
- [34] Yibing Song, Chao Ma, Xiaohe Wu, Lijun Gong, Linchao Bao, Wangmeng Zuo, Chunhua Shen, Rynson WH Lau, and Ming-Hsuan Yang. Vital: Visual tracking via adversarial learning. In *Proceedings of the IEEE Conference on Computer Vision and Pattern Recognition*, pages 8990–8999, 2018. 2, 8
- [35] Jack Valmadre, Luca Bertinetto, João Henriques, Andrea Vedaldi, and Philip HS Torr. End-to-end representation learning for correlation filter based tracking. In *Proceedings of the IEEE Conference on Computer Vision and Pattern Recognition*, pages 2805–2813, 2017. 1, 2, 8
- [36] Oriol Vinyals, Alexander Toshev, Samy Bengio, and Dumitru Erhan. Show and tell: A neural image caption generator. In *Proceedings of the IEEE Conference on Computer Vision and Pattern Recognition*, pages 3156–3164, 2015. 2
- [37] L. Wang, Y. Li, J. Huang, and S. Lazebnik. Learning two-branch neural networks for image-text matching tasks. *IEEE Transactions on Pattern Analysis and Machine Intelligence*, 41(2):394–407, Feb 2019. 1
- [38] Yi Wu, Jongwoo Lim, and Ming-Hsuan Yang. Online object tracking: A benchmark. In *IEEE Conference on Computer Vision and Pattern Recognition*, 2013. 6
- [39] Yu Xiang, Alexandre Alahi, and Silvio Savarese. Learning to track: Online multi-object tracking by decision making. In *Proceedings of the IEEE International Conference on Computer Vision*, pages 4705–4713, 2015. 1, 5
- [40] Zhengyuan Yang, Boqing Gong, Liwei Wang, Wenbing Huang, Dong Yu, and Jiebo Luo. A fast and accurate one-stage approach to visual grounding. In *The IEEE International Conference on Computer Vision (ICCV)*, October 2019. 1